Flux periodicity in superconducting rings: Comparison to loops with Josephson junctions

H. J. Fink
Department of Electrical and Computer Engineering, University of California, Davis, California 95616

V. Grünfeld
Centro Atómico Bariloche, Comisión Nacional de Energía Atómica, 8400 San Carlos de Bariloche, Rio Negro, Argentina

(Received 3 October 1985)

Two systems are described, a bare superconducting ring and a ring with an arm whose oscillatory behavior of circulating current and internal magnetic flux as a function of applied magnetic flux is remarkably similar to that of a ring with a weak link or Josephson junction. Exact closed-form solutions of the nonlinear Ginzburg-Landau equations have been found for bare rings with wire diameter $2a < \xi(t)$ and radius $R \lesssim \xi(t)$. The circulating current and internal flux dependence on the applied flux which follow from the nonlinear solutions show both nonhysteretic and hysteretic regimes depending on the size of the ring. Numerical results for the case of the ring with an arm show that for small ring sizes the critical current varies as $R^{-1/2}$ and that the node with a dangling arm (without a current) acts like a "strong link" which prevents transitions to the normal state for certain flux ranges. The results show that the periodic behavior of circulating current and internal flux in ring structures is an intrinsic quantum-mechanical feature which is not subordinate to the presence of a weak link, and thus suggests that thin wires in actual networks may supplant Josephson junctions in some instances.

I. INTRODUCTION

Arrays with nodal separations of the order of the coherence length $\xi(t)$ or smaller have recently aroused great interest for circuit applications and network equations have been developed to describe them.[1-3] For systems built of wires of diameter $2a < \xi(t)$ the order parameter may be assumed constant over each cross section and the only variation of importance is that along the wire. Thus links between nodes are treated essentially as one dimensional.

When investigating the second-order phase boundary between the normal (N) and superconducting (S) states, it is sufficient to solve the linearized Ginzburg-Landau (GL) equations. However, when dealing with the magnetic properties due to persistent currents or (critical) transport currents,[4,5] it is necessary to make use of the nonlinear GL equations.

The diamagnetic properties of de Genne's loop with a dangling arm were investigated in Ref. 6 in the context of disordered superconductors. This was done for a range of values of ring radius R $[0.1 \leq R/\xi(t) \leq 0.4]$ and for different branch lengths and it was concluded that the latter would not appreciably enhance the diamagnetic moment of the loops. However, in Ref. 4 it was shown that the critical current density of a wire with side branches increases substantially when the spacing between the nodes, L, becomes very much smaller than $\xi(t)$, and it can be proved that in this limit $[L \ll \xi(t)]$ $J_c \propto L^{-1/2}$. An increase in the critical current density of a wire array for short internodal spacings is also expected.[5]

We felt it worthwhile to study this further from a different perspective, and in this work the magnetic properties of both the bare ring and the loop with a very long arm $[L_b \gg \xi(t)]$ were investigated from the point of view of such quasi-"one-dimensional" micronetworks. When the results are compared to those of a ring containing a Josephson junction,[7] a rather surprising similarity emerges. This similarity has its origin in fluxoid quantization, which was first observed on superconducting cylinders.[8]

Both the internal flux and circulating current as obtained from the solutions of the nonlinear GL equations have a periodic dependence on the applied magnetic flux. In particular, an exact closed-form periodic solution is obtained for the bare ring. The ring with a dangling arm was solved numerically. In both cases, transitions between different quantum states are possible when sweeping the field, which, depending on the physical characteristics of the ring, may be nonhysteretic or hysteretic. All three systems: the bare ring, the ring with an arm, and the loop with a Josephson junction show similar behavior, the dangling arm being, in a sense, the opposite of a weak link (we call this a "strong" link), since, as discussed in Sec. IV, its presence inhibits transitions into the N state.

II. GENERAL THEORETICAL FRAMEWORK

In conventional units the GL equations are (see, e.g., Ref. 9)

$$\xi^2 \nabla^2 f = (f^2 + \mathbf{q}^2 - 1) f \ , \tag{1}$$

$$f^2 \mathbf{q} = (4\pi/c)(2\pi\xi\lambda^2/\phi_0)\mathbf{J} \ , \tag{2}$$

where $f(\mathbf{r})$ is the modulus of the complex order parameter $\psi = f \exp[i\varphi(\mathbf{r})]$ and $\mathbf{J}$ the current density in cgs Gaussian

units. The superfluid velocity is

$$\mathbf{q}=\xi(\nabla\varphi-2\pi\mathbf{A}/\phi_0)\ , \tag{3}$$

where $\mathbf{A}$ is the vector potential, ϕ_0 the fluxoid quantum $ch/2e$, ξ the temperature-dependent bulk coherence length, and λ the temperature-dependent bulk penetration depth. The function f^2 is proportional to the superfluid number density and it is unity when the current density and magnetic field are zero.

For our problem, it is assumed that the distances between the nodes are of order of $\xi(t)$ and that the wire diameter $2a<\lambda(t)$ and $\xi(t)$. Then the one-dimensional GL equations may be used with x being the curvilinear coordinate along the wire normalized by $\xi(t)$. When the superfluid velocity in the first GL equation is eliminated in terms of the normalized supercurrent density J by use of the second GL equation, the result in normalized form is

$$\frac{d^2f}{dx^2}+(1-f^2-J^2/f^4)f=0\ , \tag{4}$$

where $f=f(x)$ now and J is a constant. Integrating Eq. (4) once and substituting for $f^2(x)=f_0^2+t^2(x)$, where f_0 is the value of the order parameter at some extremum of $f(x)$, one obtains

$$2f^2\left[\frac{df}{dx}\right]^2=(f_0^2-f^2)[f^2(2-f_0^2-f^2)-2J^2/f_0^2] \tag{5a}$$

or

$$\left[\frac{dt}{dx}\right]^2=J^2/f_0^2-f_0^2(1-f_0^2)-(1-3f_0^2/2)t^2+t^4/2\ . \tag{5b}$$

The function $t(x)$ gives the modulation of the order parameter and is zero at the extremum. When the normalized internodal distance $L/\xi(t)$ becomes small, an approximate integration of Eq. (5b) is possible using the first two terms of the expansion of t in powers of x.

We assume that the material throughout the network is the same and homogeneous so that $f(x)$ is continuous at each node. In addition, complex current conservation[3] requires that at all nodes

$$\sum\left[\frac{i\partial\psi_n}{\partial x}+\frac{2\pi A\psi_n}{\phi_0}\right]=0 \tag{6}$$

is satisfied. Here A and ψ_n are, respectively, the vector potential along the wire and the complex order parameter at node n, and the sum is over all branches connected directly to node n.

From the real and imaginary parts of Eq. (6), one finds the following subsidiary conditions at the nodes

$$\sum\left[\frac{d\varphi_n}{dx}-\frac{2\pi A}{\phi_0}\right]\equiv\sum q_n=0\ , \tag{7}$$

$$\sum\left[\frac{df}{dx}\right]=0\ , \tag{8}$$

where q_n is the superfluid velocity entering the node, and the derivatives of $f(x)$ with respect to x are taken radially outward from the node. Equation (7) is equivalent to Kirchhoff's current law. We satisfy this by having a circulating current in the ring only while the continuity of $f(x)$ at the node is imposed. Equation (8) is an additional constraint for superconducting networks.

III. EXACT SOLUTION FOR THE BARE RING AND COMPARISON WITH THE WEAK-LINK CASE

It is possible to obtain an exact, closed-form solution for an isolated loop. If there is no node on it, all points are equivalent and $f(x)$ will be independent of the curvilinear coordinate x. Hence f will be of constant value f_0. It follows then, from Eq. (4), that

$$J=\pm f_0^2(1-f_0^2)^{1/2}\ . \tag{9}$$

The inset of Fig. 1 shows the sign convention to be used relating the positive current density J with the positive flux ϕ (right-handed system). The square of Eq. (9) is a cubic equation in f_0^2. The latter can be solved for f_0^2 in terms of J and $J_c=2/\sqrt{27}$, which is the maximum (critical) current density of Eq. (9). The relevant solution is

$$f_0^2=\tfrac{2}{3}\{\tfrac{1}{2}+\cos[\tfrac{1}{3}\cos^{-1}(1-2J^2/J_c^2)]\}\ . \tag{10}$$

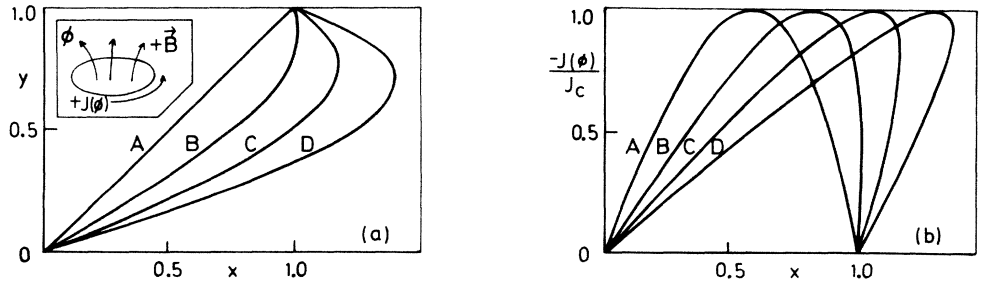

FIG. 1. Bare-ring case. (a) Plot of $y=x+\gamma J(\phi)/J_c$ [cf. Eq. (15)]. Here, $\gamma=[(1/c)LI_c/\phi_0]/(R/\xi)$, $x=(\phi_a/\phi_0-n)/(R/\xi)$ is related to the applied flux and $y=(\phi/\phi_0-n)/(R/\xi)$ is related to the total internal flux. (b) Plot of the normalized current density $-J(\phi)/J_c$ versus reduced applied flux x. Curves A, B, C, and D correspond, respectively, to values of $\gamma=0$, 0.25, 0.5, and 0.75 in both plots.

The fluxoid relation, obtained from a contour integration of the second GL equation, is

$$n\phi_0=\phi+\frac{\phi_0}{2\pi}\oint\frac{\mathbf{J}\cdot d\mathbf{x}}{f^2(x)}\ , \tag{11}$$

where n is a positive or negative integer or zero, $f(x)=f_0$, ϕ is the internal (total) magnetic flux enclosed by the contour, and

$$J=qf^2=(4\pi/c)(2\pi\xi\lambda^2/\phi_0)J_{\rm conv}\ ,$$

with $J_{\rm conv}$ the current density in conventional Gaussian units (statamperes/cm^2). Note that $\mathbf{x}$ is normalized by $\xi(t)$ in Eq. (11).

Combining Eqs. (9)–(11) and eliminating f_0, the appropriate solution for the circulating current density $J(\phi)$, as a function of the internal flux ϕ, is, in conventional units,

$$\frac{J(\phi)}{J_c}=-\frac{1}{\sqrt{2}}\left[1-\cos\left\{3\cos^{-1}\left[1-\frac{3}{2}\left[\frac{\phi/\phi_0-n}{R/\xi}\right]^2\right]\right\}\right]^{1/2}\ . \tag{12}$$

Furthermore, the internal flux as a function of the applied (external) flux ϕ_a and circulating current $I(\phi)$ (Gaussian units) is

$$\phi=\phi_a+(1/c)LI\ , \tag{13}$$

where L is the self-inductance of the loop. In order for the second term on the right-hand side to be physically meaningful, the wire of the loop must have a finite cross-sectional area of radius a. Then the current $I(\phi)=\pi a^2 J_{\rm conv}$ should be interpreted as the net circulating current in the ring whose maximum value is

$$I_c=(2/\sqrt{27})(c/4\pi)(\phi_0/2\pi\xi\lambda^2)(\pi a^2)$$

and the path of the contour integral in Eq. (11) is to be taken along the middle of the wire. Defining

$$\begin{aligned}\gamma&=[(1/c)LI_c/\phi_0]/(R/\xi)\ ,\\ x&=(\phi_a/\phi_0-n)/(R/\xi)\ ,\\ y&=(\phi/\phi_0-n)/(R/\xi)\ ,\end{aligned} \tag{14}$$

we obtain, with Eqs. (12) and (13), a relation between the applied and internal fluxes with γ as a parameter,

$$x=y-\gamma J(\phi)/J_c\ , \tag{15}$$

where $\gamma R/\xi$ is the fraction of the maximum flux generated by the circulating current in units of the fluxoid quantum. When $\gamma=0$, there is no circulating current and the applied and internal fluxes are the same; otherwise they are, in general, different.

With the above definition of y, Eq. (9) can also be written as

$$J(\phi)/J_c=-(\sqrt{27}/2)y(1-y^2)\ . \tag{12'}$$

Equations (12') and (15) give the universal relations of the internal flux and circulating current as a function of the applied flux (in terms of R/ξ and γ), which are shown in Figs. 1(a) and 1(b).

It should be pointed out that the ratio $I/I_c=J/J_c$ exists as a limiting curve for $\gamma=0$ in Fig. 1(b), although the actual circulating current approaches zero for this parameter value. In case that $\gamma\to 0$, the value of $\phi\to\phi_a$ ($y\to x$). Then y can be replaced by x in Eq. (12'). This equation shows that the current density has a maximum at $x=1/\sqrt{3}$ [Fig. 1(b), curve A]. The absolute value of the right-hand side (rhs) of Eq. (12') is similar to the Josephson $\sin(\pi y)$ relation (but not identical), where πy has to be interpreted as the phase difference across the junction. It has been shown previously,[10] in the context of S-N-S junctions, that the $\sin(\pi y)$ relation is obtained from the GL equations in the *weak*-coupling limit only. It is therefore not too surprising that Eq. (12') is not identical to the assumed $\sin(\pi y)$ relation. The periodic nature of the circulating current and flux is evident from Fig. 1 and Eqs. (15) and (12'). The functions x and J/J_c are odd functions of y.

Figure 2 shows the relation between the internal flux ϕ and the circulating current density J as a function of the applied flux ϕ_a, calculated from Eqs. (12) and (15) for quantum numbers $n=0$, 1, and 2. In all instances, the maximum flux generated by the current is fixed to $\frac{1}{4}$ of a fluxoid quantum. This requires that γ, which is proportional to the self-inductance, has to be changed as R/ξ is changed. As can be readily seen from Fig. 1, as the value of $(1/c)LI_c/\phi_0$ approaches zero, the ϕ-versus-ϕ_a and the I-versus-ϕ_a curves becomes nonhysteretic, while, for the values shown in Fig. 2, they are hysteretic. For the smaller values of R/ξ, there are regions of ϕ_a over which the ring is in the normal state while for the larger values of R/ξ the ring is always superconducting. In the graphs shown here, the current density $J(\phi)=0$ for $\phi_a=n\phi_0$, at which value the order parameter is unity in Eq. (9), while for $\phi_a=(n\pm R/\xi)\phi_0$ the values of J and f_0 are zero. For the larger values of R/ξ and when the curves bend backwards (hysteretic regime), as shown, the situation with $f_0=0$ might not ordinarily be attainable since the current in the ring switches to a different quantum state before f_0 becomes zero. At the extrema of the currents, $f_0=\sqrt{2/3}$.

From Eqs. (12) or (12') and Figs. 1 and 2, the periodic nature of J versus ϕ_a and the different quantum states are evident. Comparing the above figures with Figs. 2 and 3 of Silver and Zimmerman,[7] which concern a superconducting ring with an incorporated Josephson tunneling junction, one finds a remarkable similarity. In Ref. 7 it is the critical current of the weak link which lowers the intrinsic maximum current of the ring and thus initiates an abrupt transition to another quantum or to the normal state before the intrinsic maximum current density is reached. If the critical current of the weak link is much smaller than the intrinsic maximum current of the ring (without a weak link), then we expect the I-versus-ϕ_a and

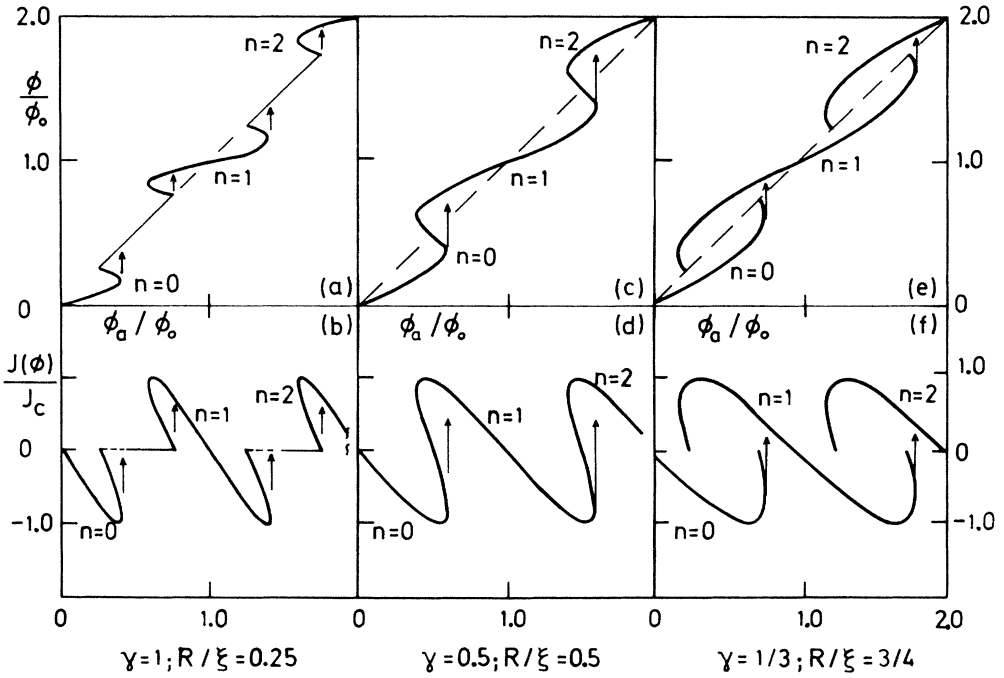

FIG. 2. Bare-ring case. Internal flux ϕ and circulating current density J as a function of the applied flux ϕ_a for $n=0$, 1, and 2 for different γ values and $\gamma R/\xi$ fixed at 0.25, obtained from Eqs. (12) and (15). Figures 1 and 2 should be compared with Figs. 2 and 3 of Ref. 7.

ϕ-versus-ϕ_a relations to be quasilinear for constant values of n. In contrast, for a bare ring the transition is determined in a natural way by the nonlinear J-versus-ϕ_a relation for smaller rings or possibly by energy-balance relations for larger rings. However, the strikingly similar behavior with and without a Josephson junction (JJ) would suggest to us that for some circuit applications a ring with a JJ could be replaced by a bare loop, a great simplification from a practical point of view.

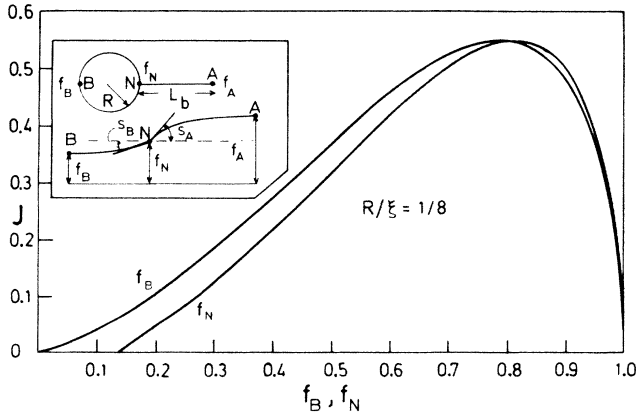

FIG. 3. Ring with a dangling arm. The inset sketches the order parameter at different locations on the ring (node N, arm A, and antinodal point B) as well as the slopes at N. The graph shows the relation between the circulating current density J and the values of f_B and f_N for $R/\xi=0.125$.

IV. NUMERICAL RESULTS FOR A RING WITH A VERY LONG ARM

When a long dangling superconducting branch, which does not carry any current, is connected to a loop, the junction (node) becomes a unique point on the ring. In contrast to the previous example, the modulus of the order parameter on the ring will now be a function of x. Also, while previously the maximum normalized current density was always $J_c=2/\sqrt{27}$, the dangling branch aids superconductivity at the node in the case of the ring with an arm, thus enhancing the maximum current. The inset of Fig. 3 shows schematically the ring with an arm and the order parameter along it.

Since the branch length $L_b \gg \xi(t)$, the order parameter $f(x)$ at point A is unity and must be a minimum at point B when a current is flowing in the loop. This follows from Eq. (8), assuming symmetry, and the assumption that $f(x)$ is continuous at the node.

When a weak link is inserted into a loop its location becomes a unique point, similar to our node. However, while the weak link initiates a transition to another quantum state before the intrinsic critical current of the bare ring is reached, the node with the arm performs the opposite function: it enhances the critical current of the system.

Because of symmetry the nodal condition, Eq. (8), for the ring with an arm, is

$$2s_B+s_A=0\ , \tag{8'}$$

where $s_A=(df/dx)_N$ is the slope at f_N going toward A

(positive) while s_B is that going toward B (negative).

When $R \ll \xi$ we may neglect the t^2 and t^4 terms on the rhs of Eq. (5b). Then the solution is

$$[J^2/f_B^2 - f_B^2(1-f_B^2)](\pi R)^2 \simeq f_N^2 - f_B^2 .$$

For the arm we use Eq. (5a) with $f_0=1$, $f=f_N$, and $J=0$. Matching the f values at the nodes and using Eq. (8'), one obtains, in the limit that $R/\xi \ll 1$, an equation for the normalized current density whose maximum value is[11]

$$J_c = \tfrac{1}{5}[3\xi(\tfrac{6}{5})^{1/2}/2\pi R]^{1/2} \simeq 0.145\sqrt{\xi/R} . \quad (16)$$

Equation (16) shows that the current density at small radii becomes quite large since the help the loop receives from the long branch becomes proportionately larger as the radius R is decreased.

The opposite extreme is when $R \gg \xi$. Then the contribution from the increased order parameter at the node is relatively small and the maximum current density in the ring approaches the value $2/\sqrt{27}$ of a very long wire without side branches.

For arbitrary values of R, however, Eqs. (4) or (5) with the boundary condition (6) and continuity of $f(x)$ at the node have to be solved numerically. Solutions were found explicitly in terms of Jacobian elliptic functions. As an example, Fig. 3 shows the relation between the values of the order parameter at points B and N and the circulating current density for $R/\xi=0.125$, and Fig. 4 shows the corresponding relation between the normalized current density and the internal flux obtained from Eq. (11) for various values of R.

The behavior of the order parameter as the current varies is quite similar to the bare-ring case, although $f(x)$ is now a function of position. It is unity at zero current, decreases as J increases and reaches a maximum value, and then decreases further until J approaches zero again. When this happens, the order parameter becomes zero at point B but has a finite value at the node N. This pattern is consistently maintained, and f_N takes on larger values with increasing values of R when $f_B=0$.

This suggests that the antinodal point B acts like a phase-slip center at which transitions from states n to $n\pm1$ might take place when $\phi_a = n\phi_0/2$. This could, for example, happen for such cases as in Figs. 5(a) and 5(b), but not in Figs. 5(c) and 5(d), where the state with $f_B=0$ is not truly accessible.

Starting from large values of f_N, J increases with ϕ until it reaches a maximum value and then drops until it becomes zero at $\phi/\phi_0 - n = 0.5$, regardless of the value of R (Fig. 4). This latter behavior is quite different from that of the bare ring, for which, when $J\to0$ and $f\to0$, the value of $\phi_a/\phi_0 \to \pm R/\xi + n$.

Defining relations similar to Eqs. (14) and (15), namely

$$\beta = (1/c)LI_c/\phi_0, \quad x = \phi_a/\phi_0 - n ,$$

$$y = \phi/\phi_0 - n, \quad x = y - \beta I(\phi)/I_c ,$$

one can calculate the internal flux ϕ and the flux generated by the circulating current $\beta I/I_c$ (in units of ϕ_0) for various values of the inductance L of the ring. Examples are shown in Fig. 5 for $R/\xi=0.125$ and 0.5 and for $\beta=0$, 0.125, and 0.25. The functions ϕ and J are periodic and odd with respect to ϕ_a. Again, as in the bare-ring case, hysteresis will occur for the larger β values when the applied magnetic field is swept in opposite directions. However, there is one important difference, that of the complete suppression of the normal regime (see, e.g., Fig. 2, $R/\xi=0.25$) due to the long deadend branch. The latter result is also different from that obtained from the linearized GL equations which has the deficiency of having no solutions for certain ranges of the length of the arm [see Ref. 1, Eq. (12)].

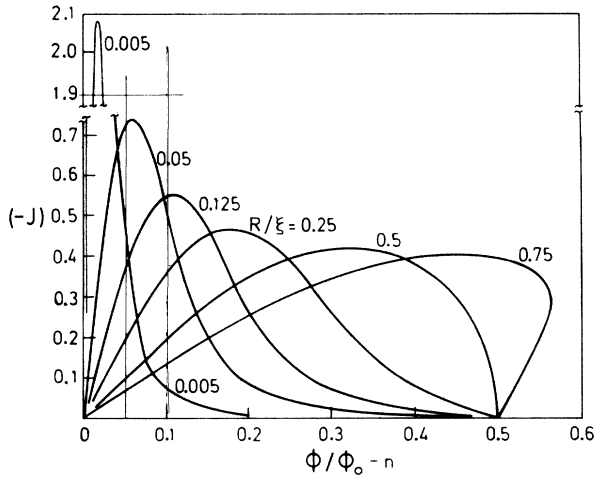

FIG. 4. Ring with an arm. Relation between the normalized current density and the internal flux obtained from Eqs. (11) and (4) for different R values with nodal condition (6) and continuity of $f(x)$ at the node.

Figure 6 shows a plot of the maximum (critical) current for the ring with an arm and the approximation for $R\to0$, Eq. (16), as a function of radius R. For large radii, $J_c \to J_c(\infty) = 2\sqrt{27}$. This value corresponds to the critical current density of a bare ring or long wire without dangling branches.

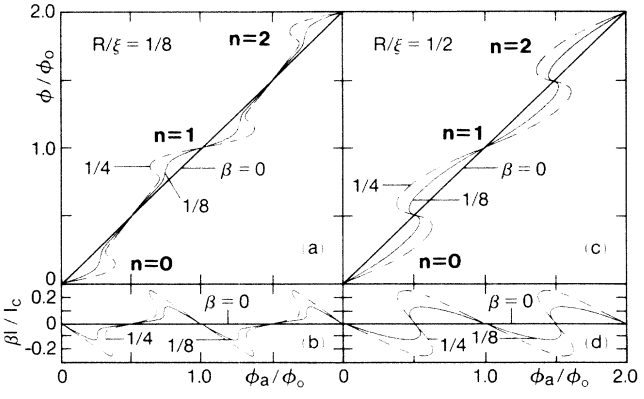

FIG. 5. Ring with an arm. Internal flux ϕ and circulating current I as a function of applied flux ϕ_a for $n=0$, 1, and 2, for different values of β $[=(1/c)LI_c/\phi_0]=0$, 0.125, and 0.25; (a) and (b) for $R/\xi=0.125$; (c) and (d) for $R/\xi=0.5$. This figure should be compared with the above Fig. 2 and with Figs. 2 and 3 of Ref. 7.

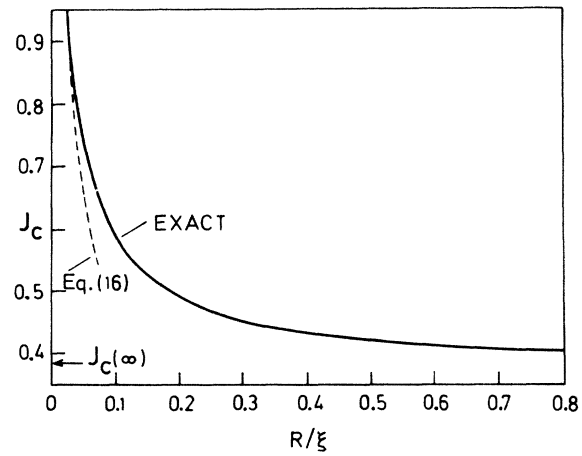

FIG. 6. Ring with an arm. Maximum (critical) circulating current is plotted as a function of R. The dashed curve is the approximation for small R values: $I_c \simeq 0.145\sqrt{\xi/R}$ [Eq. (16)].

V. CONCLUSIONS

The periodic behavior of the internal flux, locked into the ring, and that of the circulating current, as a function of the applied magnetic flux, is an intrinsic quantum-mechanical feature of a multiply connected system with a complex order parameter and not an inherent property of a Josephson junction or other type of weak link which may be part of the ring circuit. From the nonlinear GL equations, we obtained for a ring [consisting of a wire whose cross-sectional radius is smaller than $\xi(t)$], an exact closed-form solution for the circulating currents a function of the internal flux which can be related to the applied flux for a given inductance. Such a ring has an intrinsic critical current. When a weak link is inserted, it forces its own critical current upon the system, which is lower than that of the bare ring. A dangling superconducting branch produces the opposite effect: the node acts like a strong link since the critical current is raised. While rings both with and without weak links may have applied flux regions in which superconductivity is quenched altogether (e.g., see Fig. 2 for $R/\xi=0.25$), a strong link, in principle, prevents this from occurring.

The maximum current which can be sustained in a bare ring is independent of the radius R, while it is proportional to $R^{-1/2}$ for small values of R when the system includes a strong link [see Figs. 4 and 6 and Eq. (16)]. Thus for $R \to 0$ the magnetic moment varies as R^2 for a bare ring, while, for one with a strong link, it varies as $R^{3/2}$.

In summary, a bare superconducting ring [$2a < \xi(t)$, $R \lesssim \xi(t)$] shows an oscillatory behavior in the presence of an applied magnetic flux which is quite similar to that of a ring with an embedded Josephson junction. This result which follows from exact solutions of the nonlinear GL equations and fluxoid quantization raises the conjecture that wires between nodes in a superconducting network act like weak links and could replace them in some cases.

A long dangling arm without a current connected to a superconducting ring of small radius acts like a strong link since it enhances the order parameter (Cooper-pair density) and the critical current of the ring and prevents it from going into the normal state for certain applied flux ranges. Furthermore, the antinodal point B acts like a phase slip center when the quantum number is changed.

ACKNOWLEDGMENTS

We greatly appreciate the help of A. López, who critically read the manuscript. We thank Stephen M. Roberts and Joey Loo for their help with the numerical work. One of the authors (H.J.F.) acknowledges the hospitality of the members of Centro Atómico Bariloche, Argentina, where this manuscript was written and the partial support received from NSF Grants No. INT-82-13132 and No. INT-85-02375, while on leave from the University of California, Davis.

[1] P. G. de Gennes, C. R. Acad. Sci., Ser. II **292**, 279 (1981).
[2] S. Alexander, Phys. Rev. B **27**, 1541 (1983).
[3] H. J. Fink, A. López, and R. Maynard, Phys. Rev. B **26**, 5237 (1982); S. B. Haley and H. J. Fink, Phys. Lett. **102A**, 431 (1984).
[4] H. J. Fink and V. Grünfeld, Phys. Rev. B **31**, 600 (1985).
[5] H. J. Fink and A. López, J. Phys. (Paris) Lett. **46**, L961 (1985).
[6] J. P. Straley and P. B. Visscher, Phys. Rev. B **26**, 4922 (1982).
[7] A. H. Silver and J. E. Zimmerman, Phys. Rev. **157**, 317 (1965).
[8] W. A. Little and R. D. Parks, Phys. Rev. Lett. **9**, 9 (1962); R. D. Parks and W. A. Little, Phys. Rev. **133**, A97 (1964); R. P. Groff and R. D. Parks, *ibid.* **176**, 567 (1968); B. S. Deaver, Jr. and W. M. Fairbank, Phys. Rev. Lett. **7**, 43 (1961); R. Doll and M. Näbauer, *ibid.* **7**, 51 (1961); W. L. Goodman, W. D. Willis, D. A. Vincent, and B. S. Deaver, Jr., Phys. Rev. B **4**, 1530 (1971); H. J. Fink and V. Grünfeld, *ibid.* **22**, 2289 (1980).
[9] M. Tinkham, *Introduction to Superconductivity* (McGraw-Hill, New York, 1975).
[10] H. J. Fink, Phys. Rev. B **14**, 1028 (1976).
[11] B. Pannetier (private communication).